Dynamic Analysis of the Maglev Conveyor for LCD Glass Cassette

Ki-Jung Kim, Hyung-Suk Han and Chang-Hyun Kim
KIMM, Dept. of Magnetic Levitation and Linear Drive, Daejeon 305-343, KOREA
kkj74@kimm.re.kr, hshan@kimm.re.kr,chkim78@kim.re.kr

Chang-Woo Lee
Evertechno, FPD Equipment Business Team, Asan-City, Chungnam, 336-863, KOREA
leecw@evertechno.co.kr

ABSTRACT: Modeling and simulation based on virtual prototyping has been widely used in industry to decrease the cost of development. However, the application of virtual prototyping to Maglev conveyors has not been done, because the modeling and simulation technology of the Maglev conveyor based on virtual prototyping is not well established. Therefore, a dynamic model of the Maglev conveyor for carrying LCD glass cassette was developed to predict and improve levitation stability. The mechanical components, joints, and force elements are represented by multibody dynamic modeling techniques. The electromagnets and their control systems are also included in the mechanical model. With the coupled model, the dynamic responses are predicted and analyzed. In addition, the effects of the levitation control algorithm on stability are also simulated.

1 INTRODUCTION

During the last decade, the display industry has made great strides. Most of all, LCDs are now widely used in digital devices such as TVs, computer monitors, and many handheld devices. In general, the clean class of display technologies should be kept high. However, it is difficult to maintain a high clean class with the contact-type conveyor system that is currently in use. Therefore, it is important to decrease the particles generated, because LCD panels are more likely to have defects than most semiconductor ICs due to their larger size. As friction between wheels and tracks is the main source of generated particles in conventional conveyor systems, a magnetically levitated suspension can be a good solution for this.

Modeling and simulation based on virtual prototyping has been widely used in industry to decrease the cost of development. However, the application of virtual prototyping to Maglev conveyors has not been done, because the modeling and simulation technology for a Maglev conveyor based on virtual prototyping has not been established. In this paper, a dynamic model of the Maglev conveyor for carrying an LCD glass cassette is developed to predict and improve levitation stability. The mechanical components, joints, and force elements are represented by multibody dynamic modeling techniques. The electromagnets and their control systems are also included in the mechanical model. With the coupled model, the dynamic responses are predicted and analyzed. In addition, the effects of the levitation control algorithm on stability are also simulated.

The organization of this paper is as follows. In section II, the dynamic model and levitation system of the developed system will be described. In section III, some simulation results will be given to show the levitation and position control performances. Finally, section IV concludes this paper.

Figure 1. Maglev conveyor system.

The test vehicle consists of a single 5-meter chassis unit (a complete urban vehicle is comprised of two 5-meter chassis units). The full-scale test chassis and its relation to a complete vehicle are shown in Figure 2.

2 MODELING

2.1 Mechanical System

Figure 1 shows a Maglev conveyor system. The configuration is similar to that of the maglev train, in which the rail structure is surrounded by the levitation support. To reduce power consumption, permanent magnets (PM) as well as electromagnets (EM) are used. In the middle of the vehicle, a linear induction motor (LIM) is installed to thrust the vehicle by the electromagnetic induction force. In addition, guide rollers are employed to prevent collision between the LIM and the rail. Figure 2 shows the 3-D model of the designed conveyor vehicle for dynamic simulation.

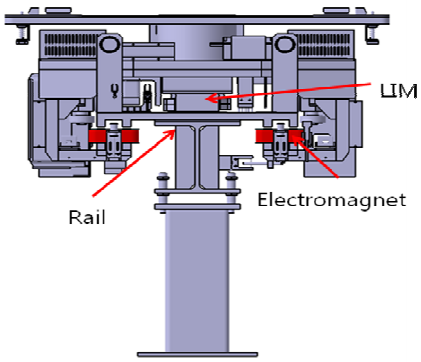

(a) Front view.

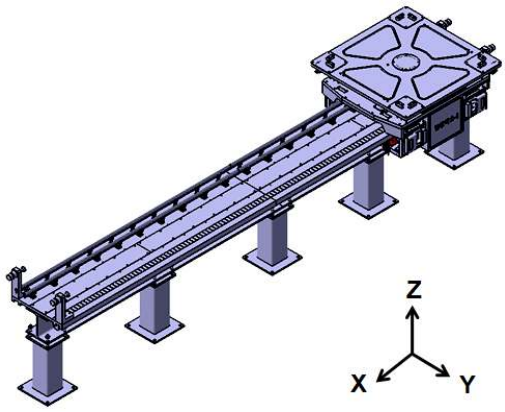

(b) Isometric view.

Figure 2. Dynamic model for Maglev conveyor system.

A procedure for dynamic simulation is shown is Fig. 3. The paper uses LMS Virtual.Lab Motion as a dynamic analysis tool for generating and solving equations of motion. The important matters to be done in Figure 3 are as follows:

LMS Virtual.Lab Motion performs modeling of bodies and their geometries, joints, suspension, and levitation control systems, and specifies the initial conditions for dynamic simulation. Equations of the magnetically-levitated system that will be given in the next section are defined in the user-defined subroutine of LMS Virtual.Lab Motion. The user-defined subroutine detects the air gap, which is the distance between an electromagnet and rail and its derivative. Then, the subroutine evaluates the system of differential equations of the levitation system, and calculates the levitation forces. The forces are applied to both the electromagnet and rail in the subroutine.

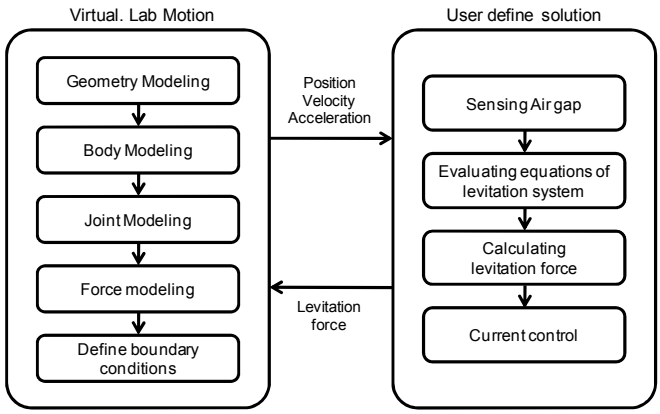

Figure 3 Process of dynamics analysis of Maglev conveyor

2.2 Levitation Control System

The levitation system consists of four EMs placed at four corners of the vehicle, and is designed to lift a 250-kg mass including a 100-kg load. Table I shows the important specifications of the designed levitation EM. The nominal gap is 3 mm, and the computed levitation force at the nominal gap is 285.34 kg.

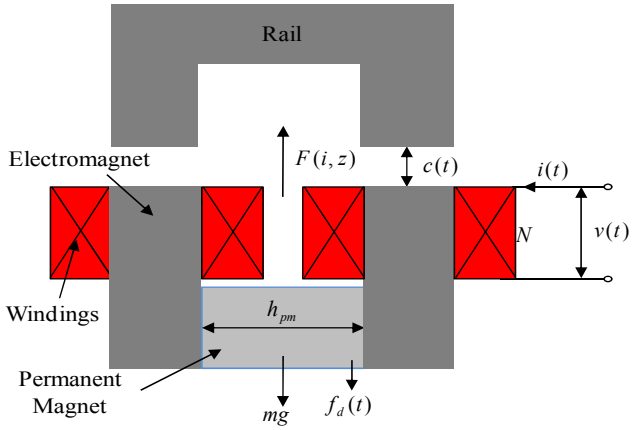

Figure 4 Simplified model of the levitation system .

TABLE I
Specifications of the Levitation Electromagnet

Items	Value
Dimension	150×20×60 (L×W×Hmm3)
Total weight	30.4kg
Nominal gap	3mm
Maximum current	±10A
Levitation weight	285.34kg (@ 0A, gap=3mm)

Figure 4 shows the mathematical model of the electromagnet. In the above figure, z denotes the length of the air gap, $f_d(t)$ is the disturbance force, and $i(t)$ is the current of coils. The attraction force $F(i(t), z(t))$, the so-called levitation force, of electromagnet suspension is expressed as Equation 1, and force is the function of the current $i(t)$ and air gap $c(t)$.

$$F = 2A\mu_0 N^2 \frac{(i(t)+i_{pm})^2}{(c(t)+c_{pm})^2} \qquad (1)$$

Here,
A = *the area of the pole*
μ_0 = *electrical coefficient*
N = *number of turns*
$i(t)$ = *current of electromagnet*
$c(t)$ = *air gap*
i_{pm} = *bias current due to permanent magnet*
c_{pm} = *bias air gap due to permanent magnet*

Figure 5 shows the estimated levitation force according to the current variation from -5A to 5A at different gaps. For example, assuming that the total weight of the vehicle is 285.43 kg, an attraction force greater than 285.43 kg can be generated by supplying 4A to the coil in order to levitate the vehicle at the landing state (5 mm gap). And, the attraction force is less than 285.43 kg by supplying -4A to the coil in order to separate the vehicle from the rail at the stuck state (1 mm gap). Therefore, the levitation control of a 285.34-kg vehicle can be achieved by supplying current within ±5A.

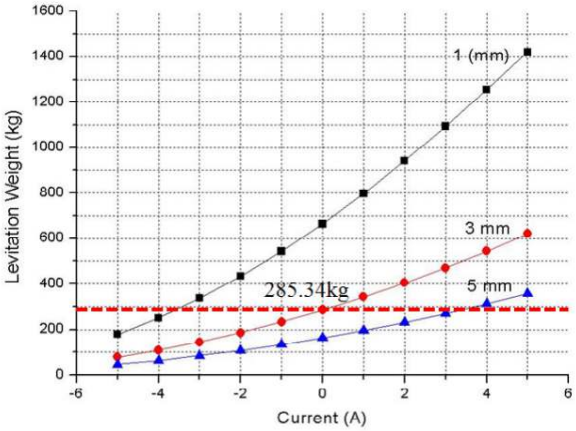

Figure 5 Levitation force vs. coil current.

This paper represented the gap $c(t)$ and the current $i(t)$ in terms of the equilibrium state, c_0 and i_0, and the displacement and the control current, $\Delta c(t)$ and $\Delta i(t)$, around it as:

$$c(t) = c_0 + \Delta c(t), \qquad i(t) = i_0 + \Delta i(t) \qquad (2)$$

Then, the equation of motion around the equilibrium position c_0 is obtained as:

$$m\frac{d^2 z(t)}{dt^2} = mg + f_d(t) - F(i(t), c(t)) \qquad (3)$$

The time delay between the commanded current and the actual current is approximated by the simplest first-order time delay model as:

$$\Delta i(t) = \frac{w_c}{s + w_c}\Delta i_r(t) \qquad (4)$$

where $\Delta i_r(t)$ is the reference current command and w_c is the cut-off frequency of electromagnet current driver. The magnetic force is obtained by using linear approximation around the nominal equilibrium point (i_0 , c_0). The resulting linear equations of the system are

$$F(\Delta c(t), \Delta i(t)) = k_c \Delta c(t) - k_i \Delta i(t) + F_0 \qquad (5)$$

Here,

$$k_i = 4A\mu_0 N^2 \frac{i_0 + i_{pm}}{(c_0 + c_{pm})^2}$$

$$k_c = 4A\mu_0 N^2 \frac{(i_0 + i_{pm})^2}{(c_0 + c_{pm})^3}$$

Then, the control current signal $\Delta i_r(t)$ is designed by the PD control theory as:

$$\Delta i_r(t) = k_P \Delta c(t) + k_D \Delta \dot{c}(t) \qquad (6)$$

The feedback gains, k_P and k_D, are designed for the linearized equation 5 by using optimal regulator theory. Then, the resulting equation for the control current is

$$\Delta \dot{i}(t) = w_c (k_P \Delta c(t) + k_D \Delta \dot{c}(t) - \Delta i(t)) \qquad (7)$$

In the determining levitation force using Equation 5 and 7, the $c(t)$, $\dot{c}(t)$ must be calculated from the position and velocity of the pair of bodies. The definition of the vertical air gap is illustrated in Fig 6. The vector between the electromagnet and the guiderail is first defined in the global reference frame as

$$\mathbf{r}_{tm} = \mathbf{r}_t - \mathbf{r}_m = \mathbf{r}_{ot} + \mathbf{A}_t \mathbf{s}'_{ot} - \mathbf{r}_{om} - \mathbf{A}_m \mathbf{s}'_{om} \qquad (8)$$

where $\mathbf{A}_t$ is the transformation matrix from guiderail to global reference frame and $\mathbf{A}_m$ is the transformation matrix from electromagnet to global reference frame.

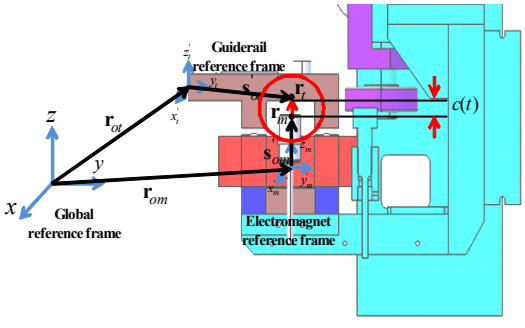

Figure. 6 Definition of vertical air gap.

Transforming the vector in Eq. (1) into the guiderail reference frame, the vector in the guiderail reference frame is obtained by

$$\mathbf{r}'_{tm} = \begin{bmatrix} x'_{tm}(t) \\ 0 \\ c(t) \end{bmatrix} = \mathbf{A}_t^T \mathbf{r}_{tm} \qquad (9)$$

The z component of the vector in Equation 9 is the $c(t)$. Differentiation Equation 8 with respect to time and transforming into the guiderail reference frame, the air gap velocity $\dot{c}(t)$ can be derived as

$$\begin{aligned} \dot{\mathbf{r}}_{tm} &= \dot{\mathbf{r}}_t - \dot{\mathbf{r}}_m = \dot{\mathbf{r}}_{ot} + \dot{\mathbf{A}}_t \mathbf{s}'_{ot} - \dot{\mathbf{r}}_{om} - \dot{\mathbf{A}}_m \mathbf{s}'_{om} \\ &= \dot{\mathbf{r}}_{ot} + \mathbf{A}_t \tilde{\boldsymbol{\omega}}'_t \mathbf{s}'_{ot} - \dot{\mathbf{r}}_{om} - \mathbf{A}_m \tilde{\boldsymbol{\omega}}'_m \mathbf{s}'_{om} \end{aligned} \qquad (10)$$

$$\dot{\mathbf{r}}'_{tm} = \begin{bmatrix} \dot{x}'_{tm}(t) \\ 0 \\ \dot{c}(t) \end{bmatrix} = \mathbf{A}_t^T \dot{\mathbf{r}}_{tm} \qquad (11)$$

To more accurately calculate the levitation force considering the relative position and orientation, the electromagnet's pole face is discretised along the length of the pole face. After calculating levitation force of each segment as shown in Figure 7, they are summed into the total levitation force on one electromagnet, and the force is applied to both the electromagnet and the guiderail.

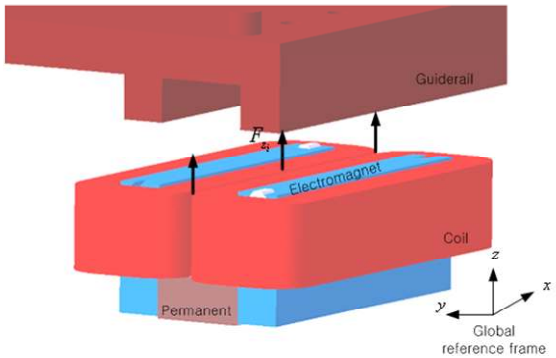

Figure. 7 Allowable guiderail profile deviations, surface roughness

C. Guiderail

The surface roughness of the guiderail interacting with the electromagnets may be restricted by specifying an allowable deviation from a datum line connecting two points. This deviation is called Versine, and is illustrated in Figure 5.

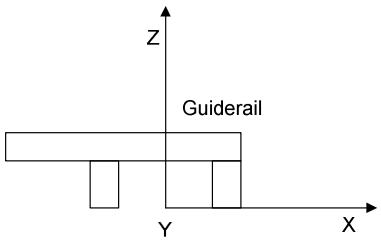

(a) Guiderail

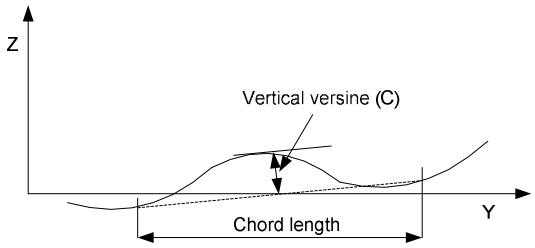

(b) Vertical versine

Figure. 8 Allowable guiderail profile deviations, surface roughness.

The generated random irregularity PSD curves are plotted in Figure 6. Allowable vertical versine is ± 2mm. The profiles are used as the guiderail elevation disturbances in the dynamic behavior predictions.

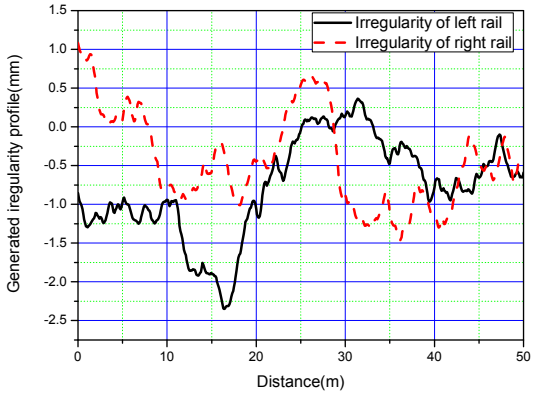

Figure. 9 Generated random irregularity profile.

.

3 SIMULATION

Using a multibody dynamic model and guiderail irregularities, the dynamic behavior prediction of the Maglev conveyor traveling on the hypothetical guiderail is carried out, and the compatibility of the proposed controller is discussed.

A. Results of test

Some experiments were performed to verify the designed control method. Experiments were carried out for 10 seconds: levitation starts at 1 second and stops at 7 seconds. In order to land off and on softly, ramp input was generated as a reference trajectory, rather than step input. Coupling between each corner is neglected, and four corners are controlled independently. The maximum load of the conveyor is 100 kg, and the experiments were performed with full load. Figure 9 shows the measured gap trajectory and the commanded coil currents for full load conditions. In the Figure 9, the measured gap is tracking the reference gap well. As expected, the commanded coil current has a small positive value near zero. The steady-state current is 1.5A, which is increased slightly again. The required current for landing on and off is less than 7A.

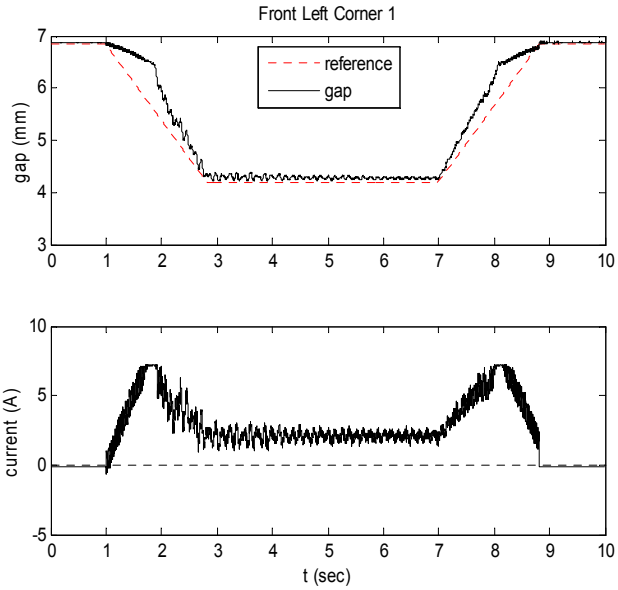

Figure. 10 Experimented levitation results (gap and commanded current).

B. Results of simulation

The simulation of the air gap, an indicator for stability, is carried out with the model of the maglev conveyor proposed in section 2. Figure 11 and 12 show air gap and levitation force time histories of 4 corners of electromagnets measured at the gap sensor during landing on. The suspension system with PM and EM is levitated steadily without contact around the nominal air gap of 3mm, and levitation force is divided equally among the 4 corners of electromagnets. Therefore, proposed dynamic model is considered reasonable.